Materials Today Bio 26 (2024) 101061

Contents lists available at ScienceDirect

Materials Today Bio

journal homepage: www.journals.elsevier.com/materials-today-bio

# 3D in vitro synovial hyperplasia model on polycaprolactone-micropatterned nanofibrous microwells for screening disease-modifying anti-rheumatic drugs

Dongwoo Kim [a], Jiyeon Heo [e], Boa Song [b], Gyubok Lee [a], Changgi Hong [a], Zhuomin Jiang [a], Sohui Lee [a], Kangwon Lee [a,d,**], Mingyo Kim [c,e,f,***], Min Hee Park [b,*]

[a] Department of Applied Bioengineering, Graduate School of Convergence Science and Technology, Seoul National University, Seoul, Republic of Korea
[b] THEDONEE Inc., Research Center, Seoul, Republic of Korea
[c] Division of Rheumatology, Department of Internal Medicine, Gyeongsang National University Hospital, Jinju, 52727, Republic of Korea
[d] Research Institute for Convergence Science, 145, Gwanggyo-ro, Yeongtong-gu, Suwon-si, Gyeonggi-do, Republic of Korea
[e] Department of Convergence Medical Science, College of Medicine, Gyeongsang National University, Jinju, 52727, Republic of Korea
[f] Department of Internal Medicine, College of Medicine, Gyeongsang National University, Jinju, 52727, Republic of Korea

ARTICLE INFO

*Keywords:*
Rheumatoid arthritis
Synovial membrane
3D spheroid
Disease-modifying antirheumatic drugs

ABSTRACT

Rheumatoid arthritis (RA) is known to be caused by autoimmune disorders and can be partially alleviated through Disease-Modifying Antirheumatic Drugs (DMARDs) therapy. However, due to significant variations in the physical environment and condition of each RA patient, the types and doses of DMARDs prescribed can differ greatly. Consequently, there is a need for a platform based on patient-derived cells to determine the effectiveness of specific DMARDs for individual patient. In this study, we established an RA three-dimensional (3D) spheroid that mimics the human body's 3D environment, enabling high-throughput assays by culturing patient-derived synovial cells on a macroscale-patterned polycaprolactone (PCL) scaffold. Fibroblast-like synoviocytes (FLSs) from patient and human umbilical vein endothelial cells (HUVECs) were co-cultured to simulate vascular delivery. Additionally, RA characteristics were identified at both the genetic and cytokine levels using real-time polymerase chain reaction (RT-qPCR) and dot blot assay. The similarities in junctions and adhesion were demonstrated in both actual RA patient tissues and 3D spheroids. The 3D RA spheroid was treated with representative DMARDs, observing changes in reactive oxygen species (ROS) levels, lactate dehydrogenase (LDH) levels, and inflammatory cytokine responses to confirm the varying cell reactions depending on the DMARDs used. This study underscores the significance of the 3D drug screening platform, which can be applied to diverse inflammatory disease treatments as a personalized drug screening system. We anticipate that this platform will become an indispensable tool for advancing and developing personalized DMARD treatment strategies.

## 1. Introduction

Rheumatoid arthritis (RA) is a chronic condition defined by complex interactions involving inflammation and autoimmune responses, characterized by the abnormal proliferation of fibroblast-like synoviocytes (FLSs) [1–4]. The primary treatment for RA involves pharmacological anti-inflammatory therapy, with surgery being considered only for cases that do not respond to medication [4,5]. Determining the correct dosage and class of RA medication is crucial for achieving the best outcomes in real-world clinical scenarios. The process of selecting and optimizing Disease-Modifying Antirheumatic Drugs must take into account individual patient characteristics, which continues to be a significant challenge [6–8].

Treating RA involves a complex process that requires consideration of individual patient characteristics and responses. The challenge of drug selection and dosage optimization is compounded without taking

* Corresponding author. THEDONEE Inc., Research Center, Seoul, Republic of Korea.
** Corresponding author. Department of Applied Bioengine-ering, Graduate School of Convergence Science and Technology, Seoul National University, Seoul, Republic of Korea.
*** Corresponding author. Division of Rheumatology, Department of Internal Medicine, Gyeongsang National University Hospital, Jinju 52727, Republic of Korea.
*E-mail addresses:* kangwonlee@snu.ac.kr (K. Lee), mingyokim1@gmail.com (M. Kim), conomo0850@gmail.com (M.H. Park).

https://doi.org/10.1016/j.mtbio.2024.101061
Received 29 December 2023; Received in revised form 10 March 2024; Accepted 13 April 2024
Available online 22 April 2024

into account the unique biological environment of each patient. Previous investigations on cells derived from patient with rheumatoid arthritis, particularly studies on the DMARD, methotrexate, have shown differential outcomes in cell viability, alanine aminotransferase levels, and mitochondrial status when testing the drug's hepatotoxicity in 3D cell cultures compared to traditional 2D flask environments [9]. Additionally, a study revealed disparities in drug resistance and dosage requirements when methotrexate was applied to both monolayer cells and 3D spheroid models of ovarian cancer cell lines [10]. Consequently, there is active research into tissue engineering designs that can mimic a patient's microenvironment, such as 3D platforms using patient-derived cells. These platforms are capable of simulating cell-cell and cell-extracellular matrix (ECM) interactions, which are difficult to replicate in two-dimensional cell cultures, such as flasks or dishes [11–13].

3D spheroids are a powerful tool for culturing single or multicellular organisms in three dimensions and mimicking the human microenvironment through ECM tuning. To date, much research has been developed for drug testing based on single or multicellular organisms [14,15]. Current studies are underway to evaluate drugs at the cellular level using patient-derived cells utilizing 3D spheroids. However, these methods, like hand drops, lack reproducibility, and using agarose with wells presents handling challenges and necrosis issues. While "organ on a chip based 3D spheroid system" can best mimic the complexity of patient sites, its engineering design and system setup are time-consuming and costly, making high-throughput testing of multiple drug types challenging [16,17]. In particular, the necrosis that occurs as the size of the spheroids increases is emerging as a challenge to long-term culture and a limitation in the application of clinical applications [18].

From this perspective, measuring the sensitivity of various types of DMARDs, mimicking the human microenvironment, and developing a 3D spheroid-based drug platform with reproducibility and cellular stability is very important. In the field of tissue engineering aimed at manipulating the 3D microenvironment, a variety of models have been developed [19,20]. Among these, the use of biodegradable and biocompatible polymers through electrospinning techniques is a widely adopted method for controlling cell adhesion, migration, and differentiation environments [21]. Electrospinning utilizes electrical forces to create fine or nanoscale fibers from polymer solutions or melts. In bioapplications, electrospinning is primarily employed for tissue engineering, drug delivery systems, wound healing dressings, tissue regeneration [22–24]. The nano and microfibers produced via this technique can mimic the extracellular matrix (ECM) of natural tissues, providing an essential 3D support structure for cell growth and differentiation. The fabricated fiber mats exhibit high porosity and surface area, which are advantageous for promoting cell attachment, proliferation, and diffusion. Biocompatible and biodegradable materials suitable for electrospinning include substances like PCL, PU, and PLLA, which can serve as ideal candidates [25,26]. Among these, PCL is FDA-approved, offering the ability to adjust its high strength and biodegradability, and can mimic complex, porous structures akin to the ECM, thus facilitating the simulation of the cell-ECM interface [27]. Therefore, we have constructed a nanofibrous microwell system using PCL-based electrospinning to mimic the cell-ECM interface. By employing patterning, we address the issue of necrosis in traditional 3D spheroids and introduce a 3D spheroid drug evaluation system that excels in cell stability, compatibility, and reproducibility.

In this study, we focused on the abnormal proliferation of FLSs in a 3D environment. The inflammatory disease environment was mimicked by activating FLSs from patient with tumor necrosis factor-alpha (TNF-α) [28]. Patient-derived FLSs were co-cultured on a micro-patterned polycaprolactone (PCL) nanofibrous scaffold with human umbilical vein endothelial cells (HUVECs) to develop an RA microenvironment that can reliably reproduce cellular spheroids. This system can be used for long-term cultures of micro-level 3D spheroids with easy media transfer. It consists of nanofibers and mimics cell-ECM interactions occurring in the human body through interactions between the PCL and cells. When testing the DMARDS, reactive oxygen species (ROS) levels, inflammatory cytokine interleukin-1 beta (IL-1β), and lactate dehydrogenase (LDH) levels were measured, determining the efficacy ranking of each drug group in five different profiles of RA patients. Fig. 1 shows synovial hyperplasia 3D spheroid model and evaluation method for DMARDs, type of drug. This study underscores the potential of a 3D drug screening platform to significantly reduce the failure rate in drug selection and increase the reliability of prescriptions when conducting patient's cell-based drug tests in the preclinical phase. It posits that such a platform will serve as a powerful tool, positively impacting the medical industry by facilitating a more informed selection of DMARDs, thereby advancing and enhancing personalized treatment strategies.

## 2. Materials and methods

### 2.1. Rheumatoid patient cell isolation and culture

Synovial fluid samples were obtained from the knee joints of patient with RA. The synovial fluid (SF) was diluted with an equal volume of Hank's Balanced Salt Solution (HBSS) and centrifuged at 2500 rpm for 20 min. The resulting pellets were resuspended in 10 mL of MEMα supplemented with 10 % fetal bovine serum (FBS) and 1 % penicillin/streptomycin, then plated in 100 mm cell culture dishes. The cultures were incubated at 37 °C in 5 % $CO_2$ for 7 days. Non-adherent cells were removed, and adherent cells were cultivated in MEMα supplemented with 10 % FBS and 1 % penicillin/streptomycin. The culture medium was replaced every 2–3 days. When the cells reached >90 % confluence, cells were harvested from the dishes by trypsinization and serially passaged (split 1:5). The purity of SF-derived FLSs was confirmed by flow cytometry analysis at passage 3. This study was conducted in accordance with the guidelines and approval of the Gyeongsang National University Hospital Institutional Review Board (IRB) (Approval No. 2019-10-021).

### 2.2. Fabrication method of the PCL-micropatterned nanofibrous microwells

PCL-micropatternd nanofibrous microwells were incorporated into hydrogel micropatterns via photolithography as described in previous study [24]. polycaprolactone (PCL) fibers were initially generated through the electrospinning method. Initially, a 20 wt% PCL solution (Molecular Weight: 80,000 g/mol, Sigma Aldrich) and 2-hydroxy-2-methylpropiophenone(HOMPP) (2 % v/v) as a photoinitiator in dissolved in 2,2,2-trifluoroethanol was extruded via a syringe pump from a 7.5 kV positive voltage-applied 18G metal needle at a consistent rate (0.8 mL/h) for a duration of 1 h. After 200 μL of precursor solution was dropped onto the electrospun fibers, a photomask containing square microarray patterns was placed on the scaffold and exposed to ultraviolet (UV) light (365 nm, EFOS Ultracure 100 ss Plus, UV spot lamp, Mississauga, ON, Canada) for 1 s to generate crosslinked hydrogel. After crosslinking, residual unreacted precursor solution was washed away with water. For cell studies, scaffolds were sterilized in 70%v/v ethanol solution for 10 min, then washed twice in phosphate buffer saline (PBS) to remove ethanol.

### 2.3. Rheumatoid patient cell seeding on the 3D macro-patterned scaffold

Human umbilical vein endothelial cells (HUVECs) were acquired from Lonza Inc. HUVECs were cultured using Endothelial Basal Medium (EBM-2, Lonza) supplemented with endothelial growth supplement single quotes (EGM-2, Lonza) and 1 % v/v antibiotic-antimycotics. Fibroblast-like synoviocytes were cultured with MEMα supplemented with 10 % FBS (Cellsera, NSW, Australia) and 1 % penicillin/streptomycin (Welgene, Korea). Each cell line was maintained in an

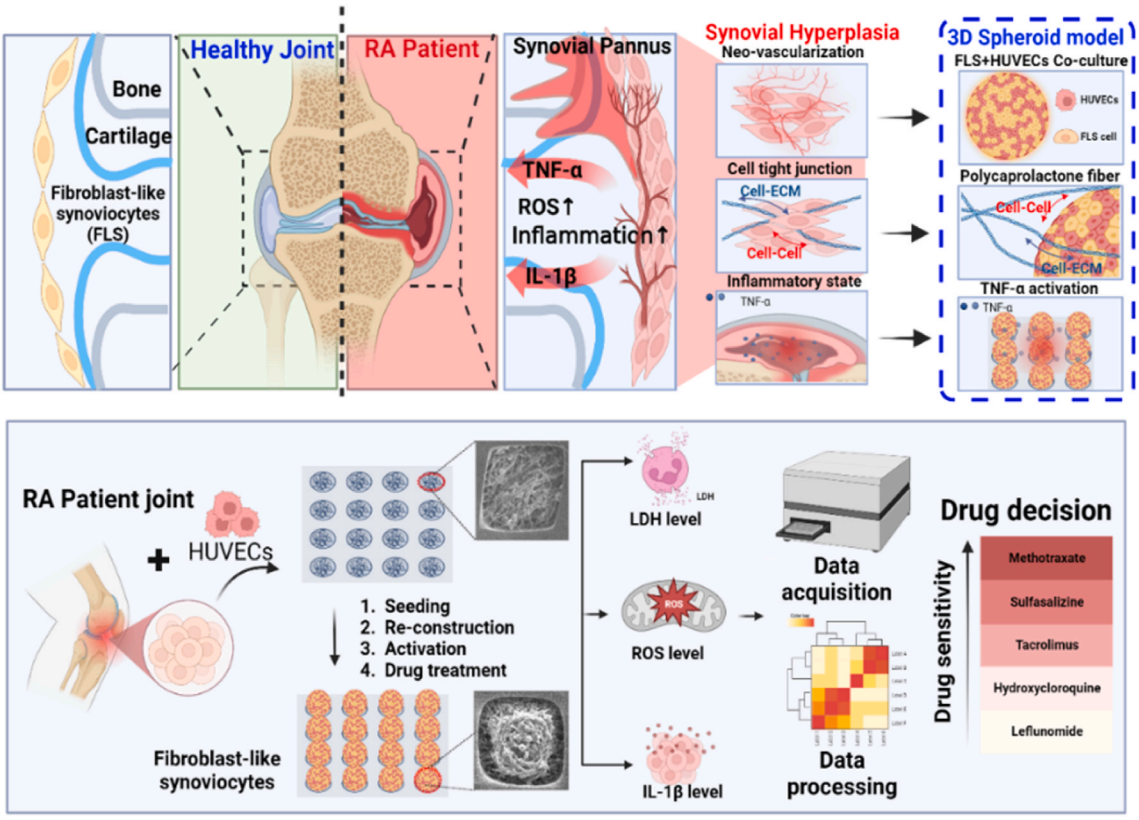


**Fig. 1.** Schematic illustration of a 3D in vitro synovial hyperplasia model simulating the rheumatoid synovial membrane. Neo-vascularization is represented using FLSs. The effects of the DMARDs are evaluated based on changes in LDH, ROS, and IL-1beta levels, highlighting drug susceptibility in actual RA patients.

environment at 5 % $CO_2$ and 37 °C. Cells were seeded on a 3D micro-pattern scaffold (TranSPHERO™) acquired from THEDONEE Inc., and DMARD testing was conducted after 4 days of culturing the spheroid.

### 2.4. Cell viability test

To assess the cell viability in co-cultured cells in 3D, $1 \times 10^5$ FLSs were seeded on a TranSPHERO™ and cultured for 1, 4, and 7 days. After treatment with 4 μM ethidium homodimer-1 (Eth-1) and 2 μM Calcein AM for 1 h, the cells were washed twice with Dulbecco's phosphate buffer saline (DPBS) and then observed under a fluorescence microscope. A laser scanning microscope (Carl Zeiss, Oberkochen, Germany) was used for fluorescence imaging.

### 2.5. In vitro cell proliferation assessment in 3D spheroids

To assess cell proliferation during the cultivation period of 3D spheroids, an in vitro cell proliferation test was conducted. Briefly, groups containing FLSs seeded in TranSPHEROTM, and co-cultured groups of FLSs and HUVECs, were seeded with a total of $1 \times 10^5$ cells. These were then cultivated over a period of 4 days. Cell proliferation was assessed by adding a water-soluble tetrazolium salt solution at 30 min before the end of the incubation period, and the absorbance was measured at 450 nm using a microplate reader (Synergy H1, BioTek, VT).

### 2.6. Immunofluorescence staining

The protein expression markers in the spheroids and patient tissues cultured in three dimensions were verified through immunofluorescent staining. The 3D spheroids and patient tissues were fixed with 4 % paraformaldehyde (Dana Korea, Korea) for 1 h and then permeabilized with Triton-X 100 at room temperature for 2 h. Staining was performed with the primary antibody overnight at 4 °C followed by the secondary antibody and then with 4′,6-diamidino-2-phenylindole (DAPI) for 15 min at room temperature. Additionally, actin filaments were stained using Phalloidin-iFluor 488 (at a 1:400 dilution, catalog number ab176753). The antibodies used included β-Actin (at a 1:500 dilution, catalog number ab227387, Abcam, UK), CD68 (at a 1:500 dilution, catalog number ab213363, Abcam, UK), EpCAM (at a 1:500 dilution, catalog number ab112067, Abcam, UK), α-sma (at a 1:500 dilution, catalog number ab5694, Abcam, UK), CD31 (at a 1:500 dilution, catalog number ab28364, Abcam, UK), CD86 (at a 1:250 dilution, catalog number B273396, BioLegend, USA), ZO-1 (at a 1:200 dilution, catalog number 40–2200, Invitrogen, USA). After the incubation with primary antibodies, the membranes were incubated with a secondary antibody Goat Anti-Rabbit IgG H&L (Alexa Fluor® 488) (at a 1:1000 dilution, catalog number ab150077, Abcam, UK), Goat Anti-Mouse IgG H&L (Alexa Fluor® 647) (at a 1:1000 dilution, catalog number ab150115, Abcam, UK).

### 2.7. Real-time quantitative polymerase chain reaction (RT-qPCR)

The gene expression level of the cells was confirmed by real-time quantitative polymerase chain reaction (real-time qPCR). For the qPCR, Thermofisher Quantastudio 5 (Applied Biosystems, USA) was used. First, TRIzol was used for 5 min to extract isolated cellular ribonucleic acid (RNA), and the RNA was purified using chloroform, isopropyl alcohol, and ethanol consecutively. Then, after quantifying the nucleic acid using NanoDrop, we synthesized cDNA with the SuperScript™ VILO™ Master Mix (Invitrogen, USA) using 1 μg of mRNA, followed by the cDNA synthesis process, lasting 99 min at 42 °C and then 5 min at 42 °C for termination. The synthesized cDNA was stored in a −80 °C deep freezer. After a denaturation process of 95 °C for 10 min,

qPCR was performed using the target primer and quantiNova SYBR Green PCR Kit (Qiagen, Netherlands). The primer sequence is described in Supplementary data.

### 2.8. Lactate dehydrogenase(LDH) assay

To evaluate the drug sensitivity of the FLSs, the amount of LDH (Dogenbio, Korea) released from the cells after drug treatment was measured. A 10 μL sample of the cell supernatant was extracted, and 100 μL of water-soluble tetrazolium salt (WST) substrate mix were incubated for 1 h at 37 °C and 5 % $CO_2$. The absorbance at 450 nm was measured using a microplate reader (Synergy H1, BioTek, VT).

### 2.9. ROS quantitative assay DCFDA/H2DCFDA assay

To measure the reactive oxygen species (ROS) level in the FLSs after DMARD treatment, a DCFDA/H2DCFDA ROS assay (Abcam, UK) was conducted. First, the cells were washed twice using DPDS, then treated with DCFDA solution, and left for 1 h. The measurement was taken at $E_x/E_m = 485/535$ nm using a microplate reader. (Synergy H1, BioTek, VT).

### 2.10. Reactive oxygen species (ROS) imaging

CellROX Green Oxidative Stress Reagent (Invitrogen, Carlsbad, CA, USA) was used to confirm intracellular ROS level. After 4 days of co-culturing patient-derived FLSs and HUVECs in 3D, peripheral blood mononuclear cells (PBMCs) were treated at concentrations of $1 \times 10^5$, $3 \times 10^5$, and $7 \times 10^5$ cells, along with a control group. CellROX Green Oxidative Stress Reagent was then directly added to 500 μL at a final concentration of 5 μmol/L. After 30 min, DAPI was added for 10 min to counterstain the nuclei. To confirm the qualitative evaluation of the intracellular ROS distribution, the labeled cells were observed using confocal laser spectroscopy.

### 2.11. Enzyme-linked immunosorbent assay (ELISA) assay

To track the cytokine levels emitted from the FLSs cultured in 3D, an enzyme-linked immunosorbent assay (ELISA) was conducted. Initially, FLSs and HUVECs were co-cultured on a 3D pattern for 4 days, followed by treatment with DMARDs and further cultured for 2 days. After this, the supernatant was collected from these cultures and centrifuged to remove any cellular debris. Post-centrifugation, IL-1β cytokines (Catalog number ab214025, Abcam, UK) were quantitatively determined using specific ELISA kits.

### 2.12. Fibroblast-like synoviocytes (FLS) activation

To activate cells derived from RA patient like an actual inflammatory environment, $1 \times 10^5$ cells were cultured on a 3D pattern for 4 days, followed by incubation with 10 ng/mL TNF-α (R&D system, USA) incubated at 37 °C and 5 % $CO_2$ for 2 days.

### 2.13. Dot blot assay using human inflammatory cytokine array

The human inflammation antibody array (Catalog number ab134003, Abcam, UK) was used for tracking multiple inflammatory cytokines released from the FLSs. Initially, FLSs and HUVECs were co-cultured in 3D for 4 days, followed by treatment with 10 ng/mL TNF-α for 2 days. The media supernatants from both treated and untreated groups were centrifuged to remove debris. Afterward, the human inflammatory cytokine array was blocked with a blocking solution for 30 min at room temperature and then incubated with the centrifuged supernatants for 2 h at room temperature. Following several washes with wash buffer, Biotin-conjugated Anti-Cytokines and HPR-Conjugated streptavidin were applied sequentially overnight at 4 °C. Finally, detection buffers C and D were mixed at a 1:1 ratio and applied to the membrane at 500 μL, and chemiluminescence detection was conducted using a Las 4000 device (Fujifilm Life Science, USA)

### 2.14. Scanning electron microscopy (SEM) imaging

After the 3D co-culturing of the FLSs and HUVECs, the resulting 3D spheroids were prepared for observation using SEM. The spheroids were fixed at 4 °C using a 2.5 % glutaraldehyde solution. Subsequently, they were treated with 2 % osmium tetroxide ($OsO_4$) for 2 h at the same temperature. Then, the spheroids were washed several times with deionized water to remove any residual staining agents. The spheroids were then dried using hexamethyldisilazane and placed in a vacuum chamber for 24 h. Finally, scanning electron microscopy images were captured using an FE-SEM Hitachi S 4100 (Hitachi, Japan).

### 2.15. DMARDs treatment and assessment of drug contribution by patient

Disease-Modifying Antirheumatic Drugs (DMARDs) such as Methotrexate (Sigma Aldrich, USA), Sulfasalazine (TCI Chemicals, Japan), Tacrolimus (MedChemExpress, USA), Hydroxychloroquine (Sigma Aldrich, USA), and Leflunomide (Hanlim pharm, Korea) were used at concentrations of 50, 25, 12.5, and 6.25 μM, respectively. Prior to each experiment, stock solutions were formulated using dimethyl sulfoxide (DMSO) and maintained at a temperature of 20 °C, the drugs were freshly diluted, ensuring that the final concentrations of DMSO remained below 0.1 %. After co-culturing FLSs derived from RA patient with HUVECs for 4 days, the cells were treated with 10 ng/mL TNF-α for 2 days to induce activation followed by treatment with the DMARDs for 2 days and then additional assay analysis (LDH, ROS(%), IL-1β). The contribution of each DMARD for a patient is denoted as $C_{total} = C_1 + C_2 + C_3 + C_4 + C_5$, where $C_{total}$ signifies the total contribution from all selected DMARDs, and $C_1$, $C_2, C_3, C_4, C_5$ represent the individual contributions of each drug, respectively. To assess the relative effectiveness of each DMARD within the treatment regimen, the percentage contribution of each drug ($P_i$) was calculated as follows: $P_i = (C_{total}/C_i)$ x 100

### 2.16. Statistical analysis

Data are presented as the mean ± standard deviation. The analysis was conducted with the aid of the GraphPad Prism 8 software (GraphPad, San Diego, CA). Group comparisons were made by one-way ANOVA, followed by multiple comparison tests with a 95 % confidence interval. Statistical significance was denoted by P-values below 0.05.

## 3. Results and discussion

### 3.1. Optimization of 3D in vitro RA model in PCL-micropatterned nanofibrous microwells

The progression of rheumatic diseases is primarily attributed to the abnormal proliferation of FLSs. Furthermore, these over-proliferative FLSs induce abnormal vascularization around them and form cell-ECM junctions [29]. In this study, a platform capable of screening DMARDs was optimized to inhibit such abnormal proliferation of FLSs. To mimic the actual human environment, 3D spheroids of an insert patterned with polycaprolactone nanofibers of TranSPHERO™ were used for simulating the ECM-Cell interactions. Additionally, HUVECs were co-cultured to mimic the abnormal blood vessels that arise with the growth of FLSs. After isolating FLSs from rheumatism patients' tissues and co-culturing with HUVECs, they were seeded on a micro-pattern that enables the formation of 3D spheroids. Fig. 2A schematically illustrates the reconstruction process that provides structural stability to the cells. The 3D spheroid platform for DMARD testing, TranSPHERO™ micro-patterned with PCL, was used for testing the DMARDs (Fig. 2. B). Furthermore, the FLSs of rheumatic patients were extracted from the synovial fluid and

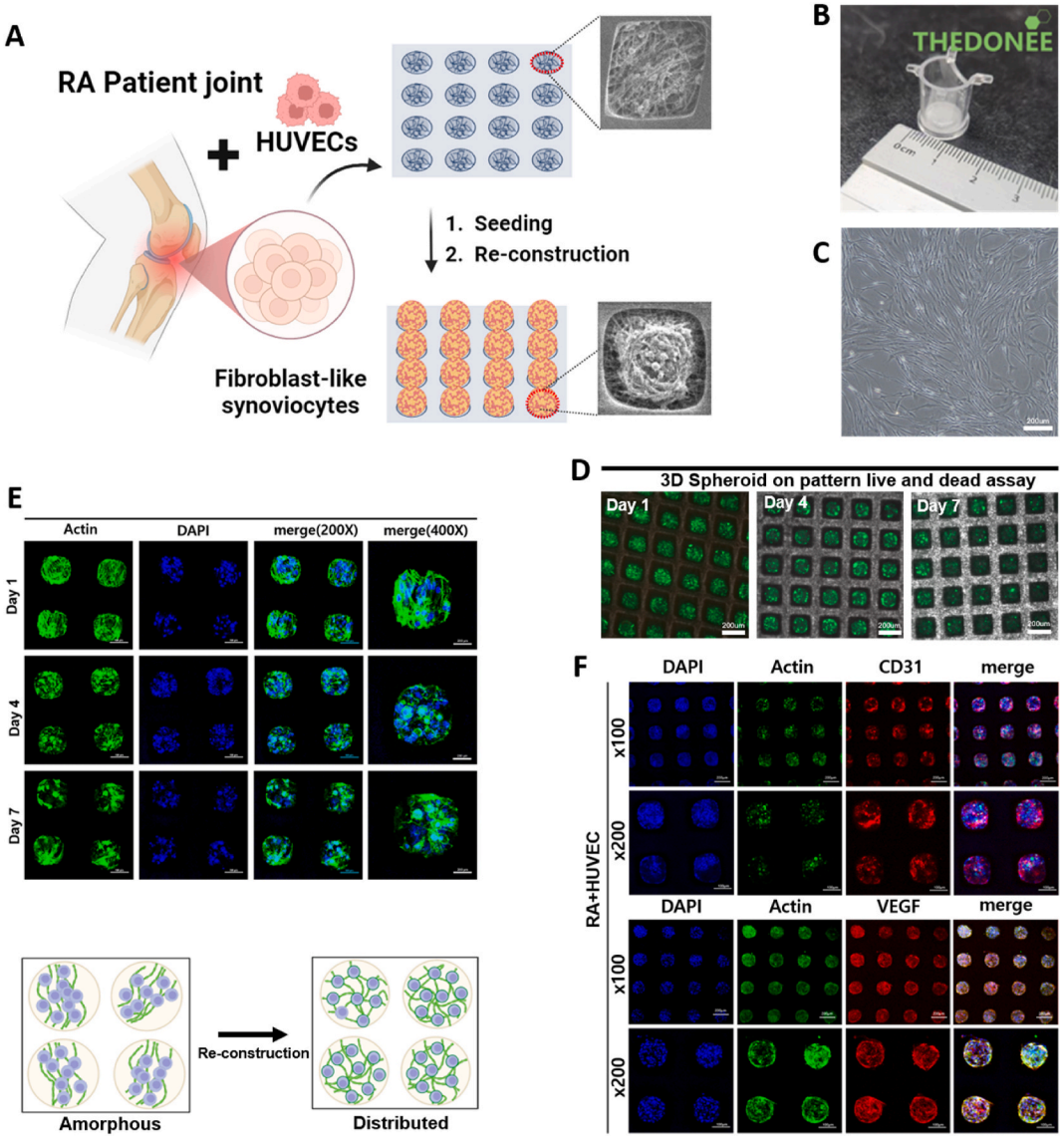


**Fig. 2.** Study on RA modeling and development of a drug screening platform to inhibit abnormal proliferation of FLSs (A) Schematic illustration representing the 3D spheroid formation process of cells derived from RA patients. (B) Image of insert micro-patterned with the PCL nanofibers of TranSPHERO™. (C) Bright-field image of FLSs extracted from the synovial fluid of rheumatoid patients. (D) Live and dead assay measuring the cell survival on a TranSPHERO™ for 1, 4, and 7 days. (E) Fluorescent imaging results of DAPI and phalloidin staining of 3D spheroids formed by patient-derived FLSs for 1, 4, and 7 days. (F) Confocal microscopy images depict the expression of CD31 and VEGF in HUVECs co-cultured with FLSs over 4 days.

used for modeling optimization and drug testing (Fig. 2. C). The biocompatibility of the FLSs on the PCL fiber patterned inserts was assessed by conducting a live and dead assay for 1, 4, and 7 days (Fig. 2. D). The results confirmed that FLSs showed no dead signal throughout the cultivation period. This result shows that there are no issues in long-term culturing and assessing drug responses based on FLSs derived from RA patients.

To confirm that the nuclei and actin had a stable structure when forming a 3D spheroid on the pattern, FLSs were cultured for 1, 4, and 7 days, followed by staining with DAPI and phalloidin, and then, fluorescent imaging was conducted (Fig. 2. E). Initially, on 1 day, actin was irregularly formed, and the nuclear placement did not interact with actin. However, from 4 days, actin formed a regular arrangement following the nucleus until 7 days. This suggests that after seeding cells to produce a 3D spheroid, more than 4 days are needed to establish a stable cellular structure. The synovial membrane shows both abnormal proliferation of FLSs and abnormal vascular hyperplasia. To mimic this, HUVECs were co-cultured with FLSs. The presence of HUVECs and vascular expression factors was confirmed through confocal microscopy by examining the expression of CD31 and vascular endothelial growth factor (VEGF) (Fig. 2. F). Overall, the presence of vascular growth factors and CD31, a membrane marker of HUVECs, was observed in the 3D spheroid. This result means that the co-culturing of rheumatic patient-derived FLSs and HUVECs successfully simulated the synovial membrane.

### 3.2. Study on rheumatoid disease modeling and development of a DMARDs screening platform to inhibit abnormal proliferation of FLSs

The characteristics of the synovial membrane of rheumatism patients are that the cell-cell interaction is very strong, and cellular activity occurs excessively [30]. In this study, a 3D spheroid mimicking the synovial membrane of rheumatoid disease was created to clarify its similarity with the synovial membrane tissue of RA patients (Fig. 3A). FLSs that promote rheumatic disease show significant differences in expression from normal fibroblasts in inflammatory responses, fibrosis,

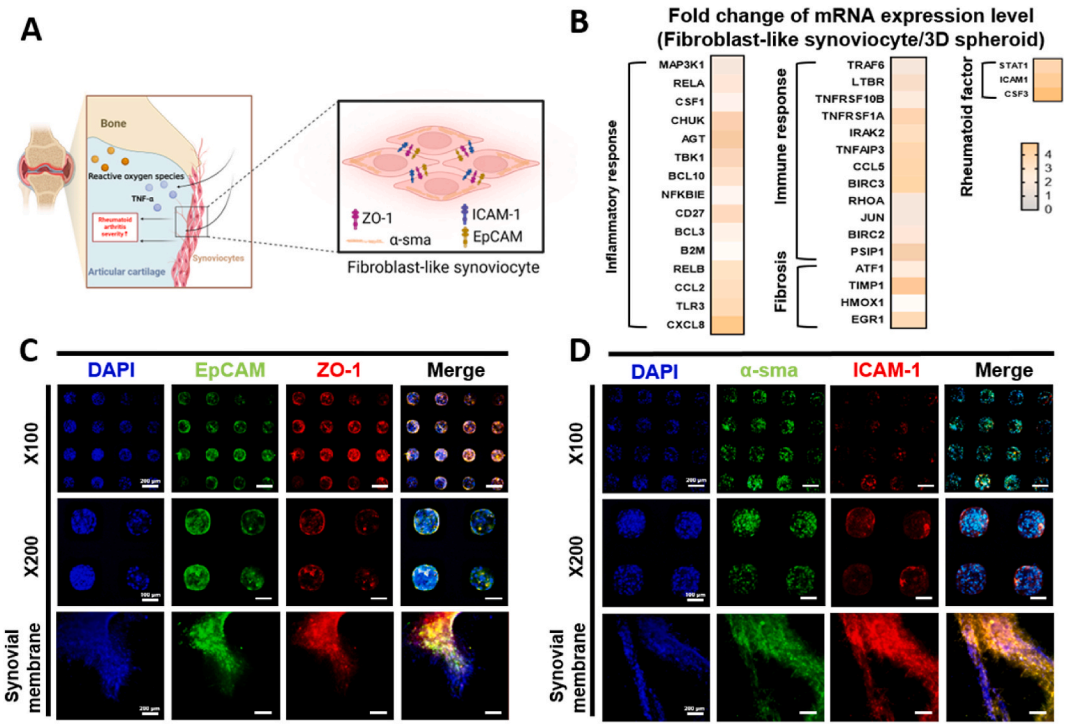


**Fig. 3.** Investigation of RA characteristics and mimicry through 3D in vitro spheroid models. (A) Schematic illustration of the rheumatoid patient's synovial membrane emphasizing strong cell-cell interactions and excessive cellular activity. (B) Gene expression differences between the optimized patient-derived 3D spheroids and normal fibroblasts highlight significant disparities in inflammatory responses, fibrosis, immune responses, and rheumatoid factors. (C) Comparison of expression patterns of ZO-1 and EpCAM in the 3D in vitro model and RA patient-derived tissue using immunofluorescence staining, revealing similarities in their patterns along cell nuclei using DAPI. (D) Comparison of expression patterns of α-SMA and ICAM-1. 3D in vitro model and RA patient tissue using immunofluorescence staining, demonstrating resemblances in their patterns along cell nuclei.

immune responses, and rheumatoid factors. In this study, the optimized patient-derived 3D spheroid was also confirmed for differences in gene expression from normal fibroblasts to determine the differences in various factors from regular fibroblasts (Fig. 3B). As a result, significant differences in expression levels were observed in the inflammatory responses, fibrosis, immune responses, and rheumatoid factors. This result confirms at the gene level that adequate modeling for rheumatism has been achieved. The similarity between the 3D in vitro model and RA patient tissue was determined through immunofluorescence staining. Among them, Zonula Occludens-1 (ZO-1) is a protein that mainly has a crucial role in cell connection and maintaining regular cell membranes. In rheumatism, ZO-1 has an essential role in the inflammatory process, regulating inflammatory signals and suppressing inflammatory responses. Moreover, epithelial cell adhesion molecule (EpCAM) regulates cell movement and interactions and affects a series of processes related to the movement of FLSs. After immunostaining the two proteins, their expression patterns were compared through fluorescence microscopy, and it was confirmed that the patterns of EpCAM and ZO-1 expressed along the nucleus were very similar (Fig. 3C). Additionally, α-smooth muscle actin (α-SMA) is a protein found in muscle cells and is associated with the fibrosis process in relation to rheumatism. Fibrosis causes tissue structure deformation due to an increase in fibrous tissue in the tissue, which can have a significant role in tissue damage diseases like rheumatism. Intercellular adhesion molecule-1 (ICAM-1) is a molecule that regulates cell-cell adhesion under inflammatory conditions and is mainly studied in inflammatory joint diseases. ICAM-1 has a critical role in regulating the adhesion and movement of inflammatory cells and the vascular endothelium associated with inflammatory and immune responses in diseases like rheumatism. After immunostaining the two proteins, their expression patterns were compared through fluorescence microscopy, and it was confirmed that the patterns of α-SMA and ICAM-1 expressed along the nucleus exhibited similar aspects (Fig. 3D). This result indicates that the properties of the FLSs existing in the synovial membrane of RA patients were well mimicked at the in vitro level.

### 3.3. *Comprehensive assessment of immune interactions and ROS level in a 3D in vitro RA model*

In rheumatic diseases, FLSs inherently exhibit hyper-proliferation and interact with immune cells. Specifically, FLSs have an intense interaction with blood monocytes such as T cells and macrophages which exacerbates inflammation. Hence, it is crucial to ascertain whether FLSs in a 3D rheumatism model interact smoothly with immune cells in three dimensions. PBMCs were introduced into a 3D spheroid model that simulates the synovial membrane in 3D. It examined the changes in ROS resulting from this introduction and the polarization of macrophages among the PBMCs and evaluated the mobility and inflammatory factors at the genetic level (Fig. 4A). First, ROS levels increased when PBMCs were introduced to the established FLS-HUVECs 3D model and were assessed using the DCFDA/H2DCFDA ROS assay (Fig. 4B). The ratios of FLSs to PBMCs were adjusted to 1:1, 1:3, and 1:7, and it was evident that the ROS levels significantly increased compared to before the PBMC treatment in the 3D FLSs and HUVECs model. Additionally, the ROS levels of the FLSs-HUVECs model influenced by the PBMCs on a 3D micro-patterned scaffold were qualitatively assessed using the Cellrox assay (Fig. 4C). Consistent with the quantitative results, the fluorescence intensity increased when the FLSs to PBMCs ratio was set at 1:1, 1:3, and 1:7 (Fig S3). These results indicate that FLSs cultured in three dimensions can reproduce the immune environment, as shown by the increased ROS levels due to the PBMCs.

Subsequently, it was confirmed by immunofluorescence whether the macrophages in PBMCs exhibit the characteristics of M1 macrophages due to the ROS environment (Fig. 4D). After staining the entirety of the

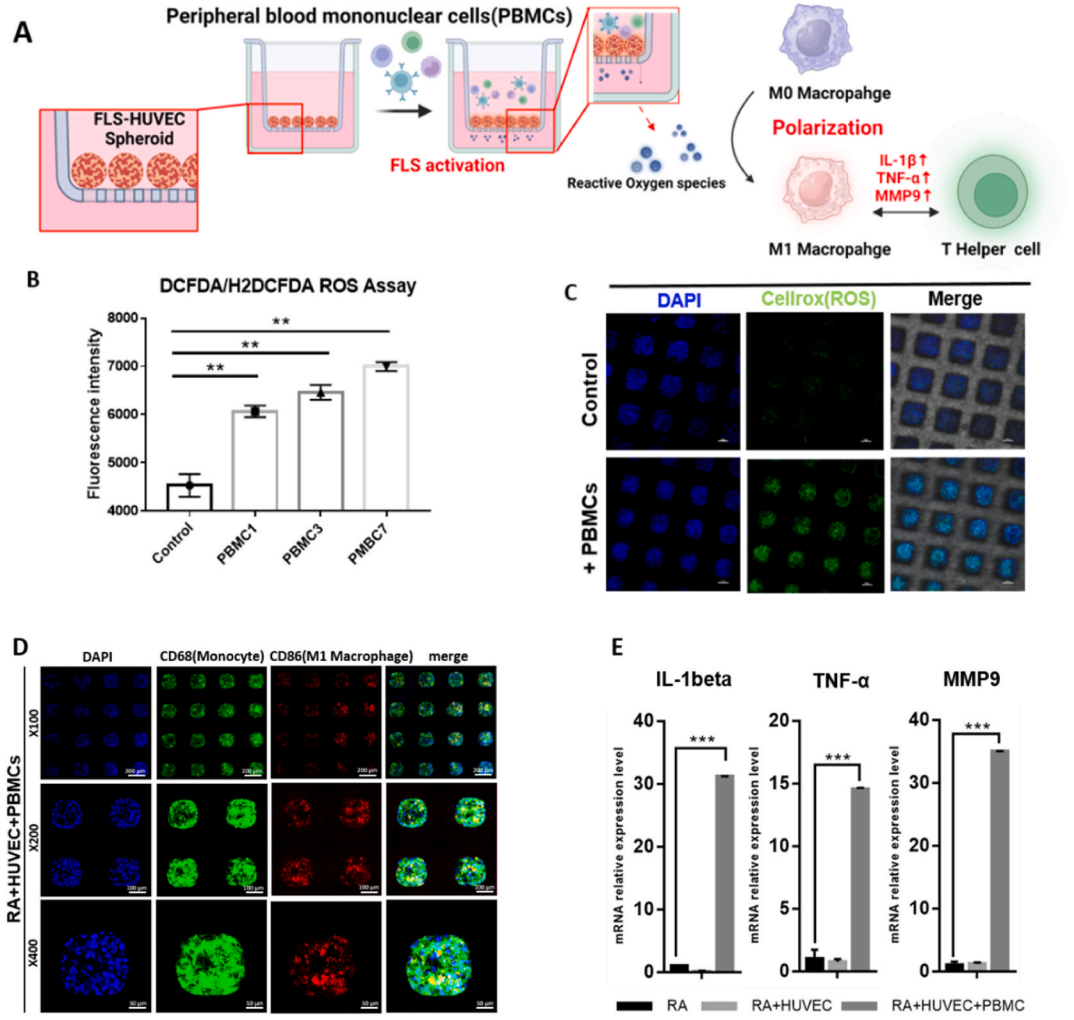


**Fig. 4. Comprehensive assessment of immune interactions and ROS level in a 3D *in vitro* RA model** (A) Schematic illustration of the evaluation of the ROS level, macrophage polarization, and inflammation-associated gene expression in the 3D spheroid model upon introducing PBMCs. (B) Quantitative assessment of the ROS levels in the FLS-HUVEC 3D model post PBMC treatment, examined with the ROS assay for various FLSs to PBMC ratios of 1:1, 1:3, and 1:7. (C) Qualitative analysis of the ROS levels in the 3D FLS-HUVEC model on a micro-patterned scaffold post-PBMC treatment, visualized using the Cellrox assay. (D) Immunofluorescence examination of macrophage polarization within PBMCs in a ROS-rich environment, characterized by CD68 staining for overall macrophage presence and CD86 staining indicative of M1 pro-inflammatory macrophages. (E) Gene expression analysis of pro-inflammatory markers IL-1β, TNF-α, and MMP9 across different cell combination groups: FLSs only, FLSs and HUVECs co-culture, FLSs and HUVECs and PBMCs tri-culture, highlighting the enhanced inflammatory response in the presence of PBMCs, *** p-value <0.0001.

PBMCs with the CD68 marker, CD86, a pro-inflammation factor for M1, was simultaneously stained, and its expression was verified. This result confirms the polarization of macrophages within the PBMCs in a ROS environment. Moreover, to determine the increased inflammation and tissue destruction resulting from the interaction between M1 macrophages and T helper cells, the gene expression levels of Interleukin-1beta (IL-1β), TNF-α and Matrix Metalloproteinase-9 (MMP-9) were measured in FLSs only, FLSs and HUVECs co-culture, and FLSs and HUVECs and PBMCs tri-culture (Fig. 4E). The results indicated no significant difference in the three factors for FLSs only and FLSs and HUVECs co-culture groups. However, in the presence of PBMCs, a considerably higher expression level was observed. These results demonstrate that our study successfully replicated the immune activity in the synovial membrane and surrounding environment of rheumatism patients.

### *3.4. Evaluating the inflammatory environment and responses of DMARDs in the 3D in vitro RA model*

The environment surrounding the synovial membrane in rheumatoid arthritis patients is characterized by an inflammatory state. Specifically, FLSs are known to enter an activated state upon exposure to high levels of TNF-α, leading to their hyper-proliferation. Previous studies involving FLSs have commonly exposed them to TNF-α to mimic this rheumatoid environment, thereby replicating the activation state [31]. In our study, we simulated the inflammatory environment using TNF-α (Fig. 5. A), and it was confirmed that FLSs exposed to TNF-α in a three-dimensional setting exhibited elevated levels of ROS and LDH level (Fig. 5. B). The increase in these two factors suggests that the activation stage of TNF-α is essential when conducting drug tests based on FLSs. Furthermore, we monitored changes in the expression of 19 genes activated by TNF-α (Fig. 5. C), among which genes related to inflammation and immunity, such as TNFRSF1A (Tumor Necrosis Factor Receptor 1), CCL2 (Monocyte Chemoattractant Protein-1, MCP-1), and NF-κB1 (Nuclear Factor Kappa B Subunit 1), showed significant increases at the genetic level. Subsequently, an inflammatory cytokine array was performed using the dot blot assay (Fig. 5. D). This assay measured cytokine levels in FLSs both before and after activation by TNF-α. The evaluation of inflammation-related factors revealed an increase in 20 different cytokines, including IFN-γ and IL-1β, with the exception of three specific factors. Additionally, among the 12 assessed chemokines, all but two

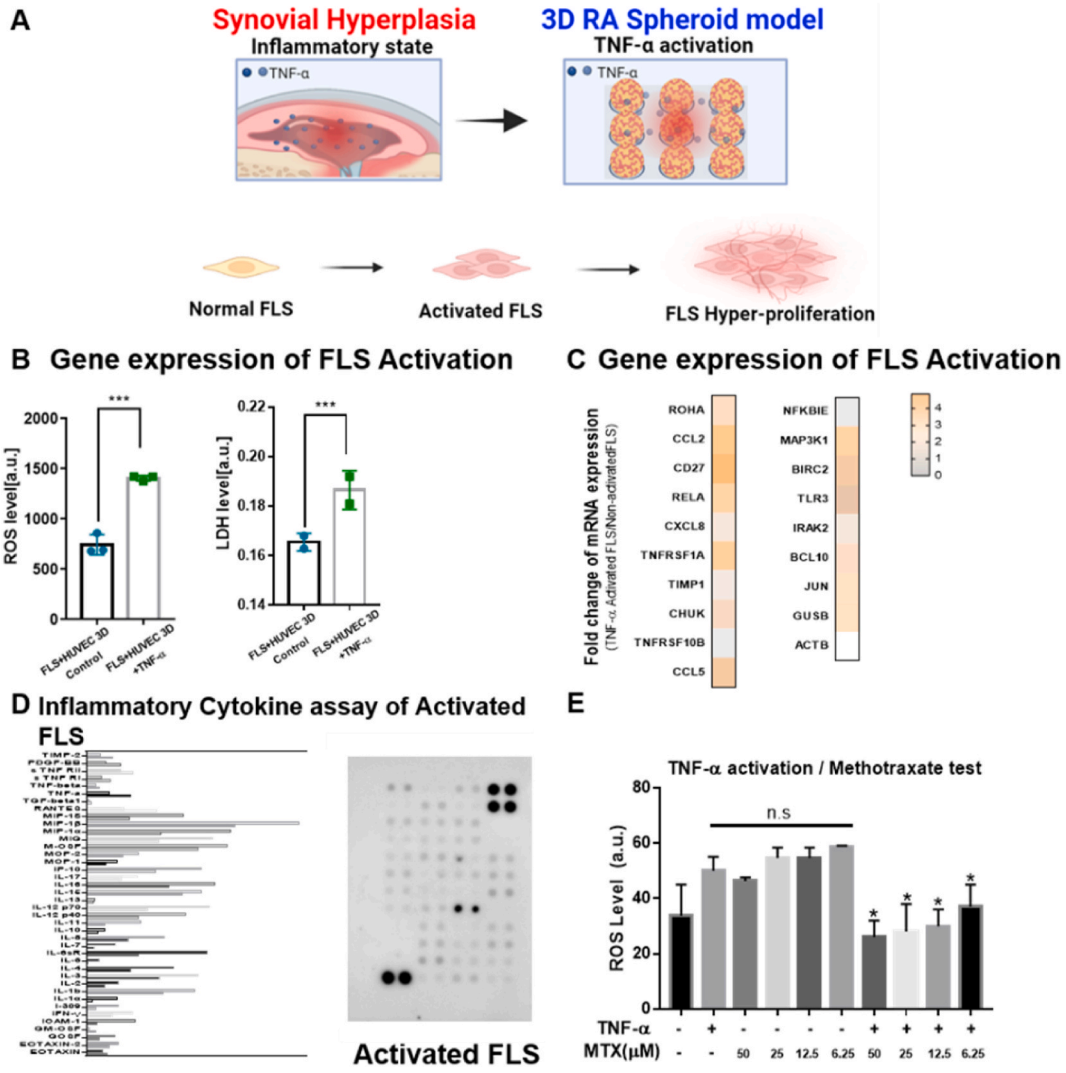


**Fig. 5.** Evaluating the inflammatory environment and DMADR response in the 3D RA in vitro model (A) Mimicking the inflammatory environment known in the rheumatoid synovial membrane using TNF-α activation in FLSs. (B) Evaluation of ROS and LDH levels in FLSs under 3D conditions upon TNF-α exposure, highlighting the hyper-proliferative nature of activated FLSs. (C) Tracking changes in gene expression in FLSs upon activation by TNF-α. (D) Examination of inflammatory cytokines using a dot blot assay. (E) Drug testing using methotrexate, a representative DMARD, both before and after TNF-α-induced activation of the rheumatoid model.

demonstrated elevated levels. This result underscores that merely culturing FLSs extracted from patients with rheumatoid arthritis does not sufficiently replicate the in vivo inflammatory environment. Finally, a drug test was conducted with methotrexate, an anti-inflammatory drug, and representative DMARDs, before and after activation by TNF-α (Fig. 5. E). To further elucidate the role of TNF-α activation in drug evaluation, we explored the effects of methotrexate (MTX), a representative Disease-Modifying Antirheumatic Drug (DMARD), at concentrations of 6.25 μM, 12.5 μM, 25 μM, and 50 μM in the context of our study. Fig. 5. E provides a detailed view of this experiment. In groups where TNF-α activation was not induced, there was no significant reduction in ROS following drug treatment. However, in groups treated with the drug post-TNF-α activation, a significant decrease in ROS levels was observed. Hence, it became clear that the rheumatoid model can not only simulate the inflammatory environment during activation but also reveal significant differences in drug behavior evaluations.

### *3.5. Assessment of the drug responsiveness of DMARDs using patient-derived FLSs on a 3D in vitro RA model*

In this study, an optimized 3D in vitro RA model was developed to assess the responsiveness of DMARDs. After extracting FLSs from actual rheumatoid arthritis patients, they were co-cultured with HUVEC cells and underwent TNF-α activation. The responsiveness to five drugs, methotrexate, sulfasalazine, tacrolimus, hydroxychloroquine, and leflunomide, was compared based on the LDH, ROS, and IL-1β levels (Fig. 6. A). After a re-construction process for cell stabilization, the DMARD drugs were administered, and the response was observed 48 h later (Fig. 6. B). First, the contribution of the LDH, ROS, and IL-1β levels to the response of each drug for individual patients was measured with a score out of 100 to determine the proportion of each response (Fig. 6. C). Subsequently, for evaluating the five drugs, the LDH, ROS, and IL-1β levels were scored from 1 to 5, and the drug responsiveness was ranked for each patient (Fig. 6. D). The results showed that out of five patients, four ranked Methotrexate as their top choice. However, for the other drugs, there was no clear trend, and the responsiveness varied. This confirms that the choice of medication in the field of rheumatoid arthritis shows great heterogeneity depending on the human body environment. At the same time, these results demonstrate that the 3D synovial membrane and inflammatory environment simulation for rheumatoid patients used in this study need to provide a suitable model to determine the actual drug responsiveness for RA patients.

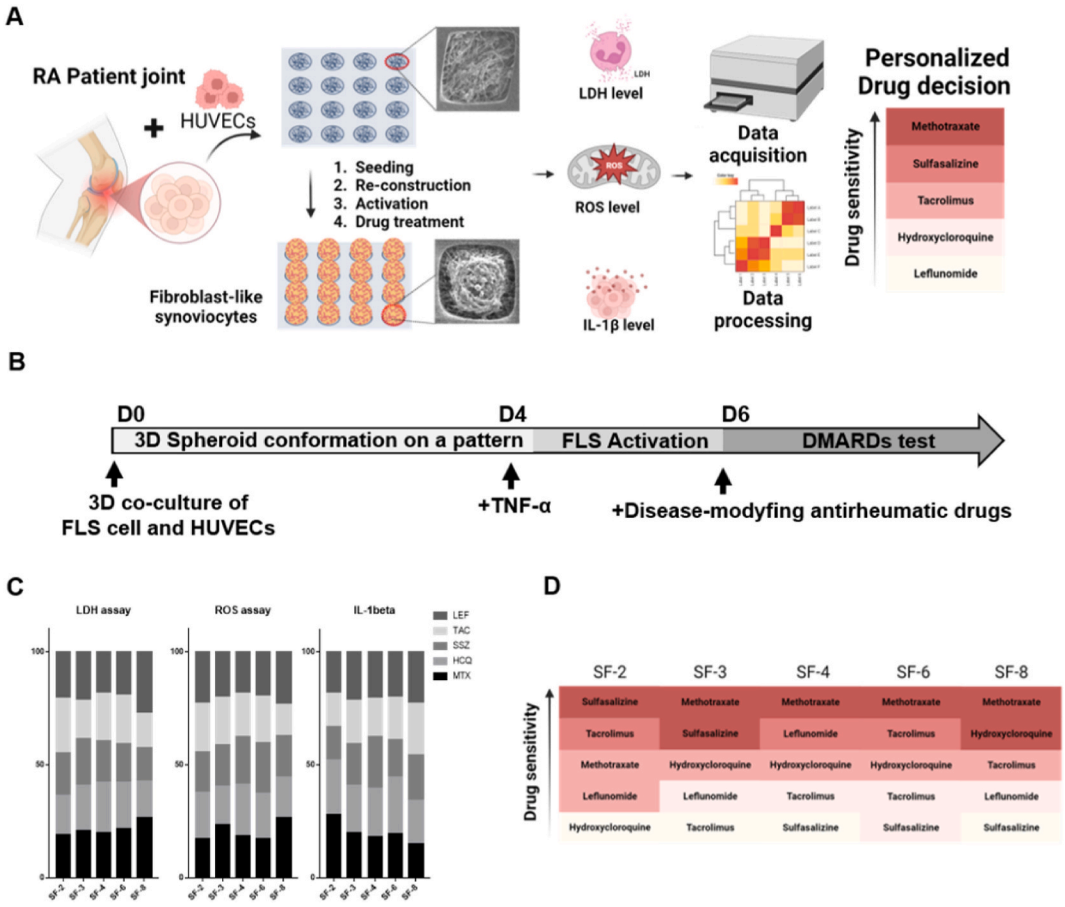


**Fig. 6. Assessment of the responsiveness of DMARDs using FLSs on the 3D in vitro RA model.** (A) Overview of the 3D RA evaluation system. RA patient-derived FLS cells were co-cultured with HUVECs, followed by TNF-α activation, and the responsiveness to five DMARDs was assessed. (B) Treatment timelines of DMARDs on the 3D RA platform using RA patient-derived cells (C) Contributions of the LDH, ROS, and IL-1β levels were quantified for each patient. (D) Responsiveness criteria were scored from 1 to 5, providing a drug sensitivity rank for each patient. Methotrexate emerged as the top choice for 4 out of 5 patients, underscoring drug selection heterogeneity in RA.

## 4. Conclusion

This research meticulously developed a 3D cell-based spheroid platform to emulate the synovial membrane in RA patients. By focusing on the abnormal proliferation of FLS in rheumatic diseases, this study established 3D spheroids that mirror the environment of RA patients. This model proved pivotal in drug screening, specifically targeting the unusual proliferation of FLSs. Key proteins, including ZO-1 and EpCAM, were identified, underscoring their roles in inflammation. The study extensively assessed immune interactions, noting heightened levels of ROS after introducing PBMCs and confirming macrophage behavior in an ROS-rich setting. The platform was further utilized to simulate inflammatory conditions using TNF-α, revealing the drug behavior of methotrexate before and after TNF-α activation. Importantly, based on real patient data, a prioritized evaluation was conducted for the responsiveness of five notable drugs, demonstrating the promising potential of the in vitro RA 3D platform for drug screening and deeper insights into RA progression and personalized treatment. This research provides a powerful tool for testing in the selection of DMARDs among RA patients, focusing on the FLSs present in synovial fluid, it's essential to note that not only the FLSs isolated from patients but also a cell-based approach is necessary for various diseases. However, for biological agents such as TNF-α inhibitors, further research is deemed necessary. These results showed the promising potential of the in vitro RA 3D platform for drug screening and deeper insights into RA progression and personalized treatment.

## CRediT authorship contribution statement

**Dongwoo Kim:** Writing – original draft, Data curation, Conceptualization. **Jiyeon Heo:** Writing – original draft, Resources. **Boa Song:** Validation, Resources. **Gyubok Lee:** Visualization, Software. **Changgi Hong:** Resources, Methodology. **Zhuomin Jiang:** Writing – review & editing, Validation. **Sohui Lee:** Formal analysis, Data curation. **Kangwon Lee:** Supervision, Project administration, Investigation. **Mingyo Kim:** Project administration, Investigation, Funding acquisition. **Min Hee Park:** Writing – review & editing, Supervision, Project administration, Investigation, Conceptualization.

## Declaration of competing interest

The authors declare that they have no known competing financial interests or personal relationships that could have appeared to influence the work reported in this paper.

## Data availability

No data was used for the research described in the article.

## Acknowledgments

This work was in part supported by the Research Institute for Convergence Science. This work was supported by the National Research Foundation of Korea(NRF) grant funded by the Korea

government(MSIT). (No. 2021R1A2C2014268 and Korea Health Industry Development Institute of the Ministry of Health & Welfare (No. HI22C1161). The funding body played an important role in the design of the study and collection, analysis, and interpretation of data and in writing the manuscript.

## Appendix ASupplementary data

Supplementary data to this article can be found online at https://doi.org/10.1016/j.mtbio.2024.101061.

## References

[1] L. Dan, Y.Y. Lv, Il-25 alleviates rheumatoid arthritis by inhibiting Th17 immune response, Ann. Rheum. Dis. 78 (2019) 288–289.
[2] Z.D. Ye, Y. Shen, K. Jin, J.T. Qiu, B. Hu, R.R. Jadhav, K. Sheth, C.M. Weyand, J. J. Goronzy, Arachidonic acid-regulated calcium signaling in T cells from patients with rheumatoid arthritis promotes synovial inflammation, Nat. Commun. 12 (1) (2021).
[3] Q. Meng, B. Pan, P. Sheng, Histone deacetylase 1 is increased in rheumatoid arthritis synovium and promotes synovial cell hyperplasia and synovial inflammation in the collagen-induced arthritis mouse model the microRNA-124-dependent MARCKS-JAK/STAT axis, Clin. Exp. Rheumatol. 39 (5) (2021) 970–981.
[4] A. Denis, C. Sztejkowski, L. Arnaud, G. Becker, R. Felten, The 2023 pipeline of disease-modifying antirheumatic drugs (DMARDs) in clinical development for spondyloarthritis (including psoriatic arthritis): a systematic review of trials, RMD Open 9 (3) (2023).
[5] Y. Tanaka, Recent progress in treatments of rheumatoid arthritis: an overview of developments in biologics and small molecules, and remaining unmet needs, Rheumatology 60 (2021) 12–20.
[6] R. Panaccione, S. Danese, W. Zhou, J. Klaff, D. Ilo, X. Yao, G. Levy, P.D.R. Higgins, E.J.r. Loftus, S. Chen, Y.S. Gonzalez, C. Leonard, X. Hébuterne, J.O. Lindsay, Q. Cao, H. Nakase, J.F. Colombel, S. Vermeire, Efficacy and safety of upadacitinib for 16-week extended induction and 52-week maintenance therapy in patients with moderately to severely active ulcerative colitis, Aliment. Pharmacol. Ther. 59 (3) (2024) 393–408.
[7] Y. Ren, Q. Yang, T. Luo, J. Lin, J. Jin, W.W. Qian, X.S. Weng, B. Feng, Better clinical outcome of total knee arthroplasty for rheumatoid arthritis with perioperative glucocorticoids and disease-modifying anti-rheumatic drugs after an average of 11.4-year follow-up, J. Orthop. Surg. Res. 16 (1) (2021).
[8] B. San Koo, S. Eun, K. Shin, S. Hong, Y.G. Kim, C.K. Lee, B. Yoo, J.S. Oh, Differences in trajectory of disease activity according to biologic and targeted synthetic disease-modifying anti-rheumatic drug treatment in patients with rheumatoid arthritis, Arthritis Res. Ther. 24 (1) (2022).
[9] J. Kim, Y. Kim, J. Choi, H. Jung, K. Lee, J. Kang, N. Park, Y.A. Rim, Y. Nam, J.H. Ju, Recapitulation of methotrexate hepatotoxicity with induced pluripotent stem cell-derived hepatocytes from patients with rheumatoid arthritis, Stem Cell Res. Ther. 9 (2018).
[10] M. Swierczewska, K. Sterzynska, M. Rucinski, M. Andrzejewska, M. Nowicki, R. Januchowski, The response and resistance to drugs in ovarian cancer cell lines in 2D monolayers and 3D spheroids, Biomed. Pharmacother. 165 (2023).
[11] K.M. Appleton, K.A. Lassahn, A.K. Elrod, T.M. DesRochers, Dissecting personalized PD-1 inhibitor efficacy using patient-derived 3D spheroids, Cancer Res. 82 (12) (2022).
[12] K.A. Lassahn, A.K. Elrod, A.L. Carlson, N.A. Dance, M. Millard, M.J. Wick, T. M. DesRochers, K.M. Appleton, Preclinical testing of therapeutic biologics using patient-derived 3D spheroids, Cancer Res. 83 (7) (2023).
[13] R.A. Anisimov, D.A. Gorin, A.A. Abalymov, 3D cell spheroids as a tool for evaluating the effectiveness of carbon nanotubes as a drug delivery and photothermal therapy agents, C-J Carbon Res 8 (4) (2022).
[14] M. Zanoni, F. Piccinini, C. Arienti, A. Zamagni, S. Santi, R. Polico, A. Bevilacqua, A. Tesei, 3D tumor spheroid models for therapeutic screening: a systematic approach to enhance the biological relevance of data obtained, Sci Rep-Uk 6 (2016).
[15] S.Y. Lee, I.S. Koo, H.J. Hwang, D.W. Lee, three-dimensional (3D) cell culture tools for spheroid and organoid models, Slas Discov 28 (4) (2023) 119–137.
[16] S. Lee, J. Lim, J. Yu, J. Ahn, Y. Lee, N.L. Jeon, Engineering tumor vasculature on an injection-molded plastic array 3D culture (IMPACT) platform, Lab Chip 19 (12) (2019) 2071–2080.
[17] D. Sekhar, E. Lisicka-Skrzek, P. Berini, Wafer-bonded deep fluidics in BCB with in-plane coupling for lab-on-a-chip applications, Micro Nano Eng 21 (2023).
[18] A. Wolff, M. Frank, S. Staehlke, A. Springer, O. Hahn, J. Meyer, K. Peters, 3D spheroid cultivation alters the extent and progression of osteogenic differentiation of mesenchymal stem/stromal cells compared to 2D cultivation, Biomedicines 11 (4) (2023).
[19] L.B. Bezek, M.P. Cauchi, R. De Vita, J.R. Foerst, C.B. Williams, 3D printing tissue-mimicking materials for realistic transseptal puncture models, J Mech Behav Biomed 110 (2020).
[20] D.G. Hwang, Y.M. Choi, J. Jang, 3D bioprinting-based vascularized tissue models mimicking tissue-specific architecture and pathophysiology for studies, Front. Bioeng. Biotechnol. 9 (2021).
[21] J. Hong, M. Yeo, G.H. Yang, G. Kim, Cell-electrospinning and its application for tissue engineering, Int. J. Mol. Sci. 20 (24) (2019).
[22] E.J. Torres-Martínez, J.M.C. Bravo, A.S. Medina, G.L.P. González, L.J.V. Gómez, A summary of electrospun nanofibers as drug delivery system: drugs loaded and biopolymers used as matrices, Curr. Drug Deliv. 15 (10) (2018) 1360–1374.
[23] C. Hong, H. Chung, G. Lee, C. Kim, D. Kim, S.J. Oh, S.H. Kim, K. Lee, Hydrogel/nanofiber composite wound dressing optimized for skin layer regeneration through the mechanotransduction-based microcellular environment, ACS Appl. Bio Mater. 6 (5) (2023) 1774–1786.
[24] H.S. Shin, Y.M. Kook, H.J. Hong, Y.M. Kim, W.G. Koh, J.Y. Lim, Functional spheroid organization of human salivary gland cells cultured on hydrogel-micropatterned nanofibrous microwells, Acta Biomater. 45 (2016) 121–132.
[25] Y.C. Chien, W.T. Chuang, U.S. Jeng, S.H. Hsu, Preparation, characterization, and mechanism for biodegradable and biocompatible polyurethane shape memory elastomers, ACS Appl. Mater. Interfaces 9 (6) (2017) 5419–5429.
[26] L. Peponi, I. Navarro-Baena, A. Sonseca, E. Gimenez, A. Marcos-Fernandez, J. M. Kenny, Synthesis and characterization of PCL-PLLA polyurethane with shape memory behavior, Eur. Polym. J. 49 (4) (2013) 893–903.
[27] M. Licciardello, G. Ciardelli, C. Tonda-Turo, Biocompatible electrospun polycaprolactone-polyaniline scaffold treated with atmospheric plasma to improve hydrophilicity, Bioengineering-Basel 8 (2) (2021).
[28] Y. Qin, M.L. Cai, H.Z. Jin, W. Huang, C. Zhu, A. Bozec, J.G. Huang, Z. Chen, Age-associated B cells contribute to the pathogenesis of rheumatoid arthritis by inducing activation of fibroblast-like synoviocytes via TNF-α-mediated ERK1/2 and JAK-STAT1 pathways, Ann. Rheum. Dis. 81 (11) (2022) 1504–1514.
[29] B. Bartok, G.S. Firestein, Fibroblast-like synoviocytes: key effector cells in rheumatoid arthritis, Immunol. Rev. 233 (2010) 233–255.
[30] T. Pap, B. Dankbar, C. Wehmeyer, A. Korb-Pap, J. Sherwood, Synovial fibroblasts and articular tissue remodelling: role and mechanisms, Semin. Cell Dev. Biol. 101 (2020) 140–145.
[31] A. Lee, G. Grigoriev, J. Chen, L.B. Ivashkiv, G.D. Kalliolias, TNFα induces sustained signaling and a prolonged and unremitting inflammatory response in synovial fibroblasts, Arthritis Rheum-Us 64 (10) (2012) S381–S382.